Mon. Not. R. Astron. Soc. **000**, 000–000 (0000) Printed 1 February 2008 (MN LATEX style file v2.2)

The Baryonic and Dark Matter Properties of High Redshift Gravitationally Lensed Disk Galaxies

P. Salucci[1], A. M. Swinbank[2], A. Lapi [1], I. Yegorova[1],
R. G. Bower[2], Ian Smail[2], G. P. Smith[3]

[1] *Astrophysics Sector, SISSA/ISAS, Via Beirut 2-4, I-34014 Trieste, Italy*
[2] *ICC, Department of Physics, Durham University, Durham*
[3] *School of Physics and Astronomy, University of Birmingham, Edgbaston, Birmingham, B15 2TT*
**Email: salucci@sissa.it*

1 February 2008

ABSTRACT

We present a detailed study of the structural properties of four gravitationally lensed disk galaxies at $z = 1$. Modelling the rotation curves on sub-kpc scales we derive the values for the disk mass, the reference dark matter density and core radius, and the angular momentum per unit mass. The derived models suggest that the rotation curve profile and amplitude are best fit with a dark matter component similar to those of local spiral galaxies. The stellar component also has a similar length scale, but with substantially smaller masses than similarly luminous disk galaxies in the local universe. Comparing the average dark matter density inside the optical radius we find that the disk galaxies at $z = 1$ have larger densities (by up to a factor of ~ 7) than similar disk galaxies in the local Universe. Furthermore, the angular momentum per unit mass versus reference velocity is well matched to the local relation, suggesting that the angular momentum of the disk remains constant between high redshifts and the present day. Though statistically limited, these observations point towards a spirals' formation scenario in which stellar disks are slowly grown by the accretion of angular momentum conserving material.

Key words: galaxies, rotation curves, galaxies, gravitational lensing, galaxy clusters, Integral Field Spectroscopy, Gravitational Arcs: Individual

1 INTRODUCTION

It has long been known that the kinematics of spiral galaxies do not show Keplerian fall-off in their rotation curves, but rather imply the presence of an invisible mass component in addition to the stellar and gaseous disks (Rubin et al. 1980; Bosma 1981; Persic & Salucci 1988). In the local Universe, observing the distribution of star light and mapping the gaseous component through HI it has been possible to build up a picture of the how the baryonic component of disk galaxies is distributed and how this relates to the underlying dark matter component (e.g. Persic et al. 1996). Tracing the evolution of galaxy mass from high-redshift up to the present day is only truly reliable if we can observe the same components at early times. A pioneering study was performed by Vogt et al. 1996 where a handful of rotation curves (RC's) of objects at $z \sim 0.5$ was obtained using traditional longslit spectroscopy on the 10 meter Keck Telescope. However, at higher redshifts (e.g. z$\gtrsim$1) galaxies are much fainter and have smaller angular disk scale lengths than galaxies observed at low redshift, therefore obtaining the spatial information required for detailed studies is beyond the limits of current technology. Indeed, mapping the internal properties and dynamics of both the stellar and gaseous components of galaxies at high redshift is one of the main science drivers for the next generation of ground and spaced based telescopes at many wavelengths (e.g. ELT, NGST, ALMA).

One way to overcome this problem is to use the natural amplification caused by gravitational lensing to boost the size and flux of distant galaxies which serendipitously lie behind massive galaxy clusters. This technique is extremely useful since we are able to target galaxies which would otherwise be too small and faint to ensure a sufficiently high signal-to-noise spectroscopy in conventional observations. As such, gravitational lensing has been extensively used to make detailed studies of distant galaxies: for a galaxy at z=1 with an amplification factor ten, an angular scale of $0.6''$ can correspond to $\lesssim$0.5 kpc, sufficient to map also a small spiral.

The benefits of gravitational lensing are complemented by Integral Field Spectroscopy (which produces a contiguous *two dimensional velocity* map at each point in the target galaxy). This allows a clean decoupling of the spatial and spectral information, thus eliminating the problems arising from their mixing in traditional long-slit observations. It is therefore much easier to identify and study galaxies with regular (bi-symmetric) velocity fields.

In this paper, we present a detailed study of four rotation curves extracted from disk galaxies which have been observed through the cores of massive galaxy cluster lenses. These targets are taken from the recent work of Swinbank et al. (2003, 2006). They were observed with the Gemini-North Multi-Object Spectrograph Integral Field Unit (GMOS IFU)[1]. We concentrate on the galaxy dynamics as traced by the [OII]$\lambda\lambda$3726.1,3728.8Å emission line doublet. The IFU data provide a map of the galaxy's velocity field in sky co-ordinates. To interpret this field the magnification and distortion caused by the gravitational lensing effect is removed using detailed models of the cluster lenses (see Smith et al. (2005), Kneib et al. (1996), Smith (2002) for details). The primary constraints on the lens models are the positions and redshifts of spectroscopically confirmed gravitational arcs in each cluster. The source plane velocity fields of four systems which display regular (bi-symmetric) rotational velocity fields i.e. resembling rotating disks, were reduced to one-dimensional rotation curves from which the asymptotic terminal velocity was extracted and compared with the galaxy luminosity (Swinbank et al. 2003, 2006). The key advantage of using gravitational lensing to boost the images of distant galaxies is that we are less biases towards the most luminous galaxies. Whilst observational information on the distribution of the HI disks in galaxies at these early times would be wellcome, such observations will have to wait for future instrumentation (e.g. ALMA).

In this paper we use nebular emission lines to probe the kinematic of the galaxies. We extract one-dimensional rotation curves from the velocity fields to infer the distribution of stellar and dark matter components. Finally, we compare our results with similarly luminous disk galaxies in the local Universe. Through-out this paper we use a cosmology with $H_0 = 72\,\mathrm{km\,s^{-1}}$, $\Omega_0 = 0.3$ and $\Lambda_0 = 0.7$, $t_0 = 13.7\ Gyr$.

2 DATA

2.1 Sample Selection

Our sample comes from observations of six gravitational arcs in Swinbank et al. (2006). In order to avoid possible biases, the targets were selected only to be representative of galaxies in the distant Universe and no attempt was made to select galaxies with relaxed late-type morphology. We did, however, require that arcs were resolved in both spatial dimensions so that a two dimensional velocity field could be extracted from the IFU data. This restricted our selection to galaxies with moderate magnification. From the sample of six galaxies, four galaxies appear to have (relaxed) bi-symmetric velocity fields with late-type morphologies and colours. The rotation curves from these four galaxies appear regular and we therefore restrict our analysis to these arcs. We stress that the morphology, colours and velocity fields of the four galaxies in this sample all strongly suggest these galaxies are consistent with late type spirals (see Swinbank et al. (2006)).

[1] Programme ID: GN-2003A-Q-3. The GMOS observations are based on observations obtained at the Gemini Observatory, which is operated by the Association of Universities for Research in Astronomy, Inc., under a cooperative agreement with the NSF on behalf of the Gemini partnership: the National Science Foundation (United States), the Particle Physics and Astronomy Research Council (United Kingdom), the National Research Council (Canada), CONICYT (Chile), the Australian Research Council (Australia), CNPq (Brazil) and CONICET (Argentina).

PROPERTIES OF THE GALAXIES

Arc	z	M_D (10^{10} M$_\odot$)	r_0 (kpc)	ρ_0 (10^{-23}g cm^{-3})	R_{opt} (kpc)	v_{0h} (km s^{-1})
A2390	0.912	0.40	3.1	1.4	8.3	151
RGB1745	1.056	0.18	4.2	0.37	9.6	104
A2218	1.034	1.70	5.8	0.64	7.7	166
Cl2236	1.116	0.12	1.4	3.2	5.4	101

Table 1. Derived structural parameters from the RC mass modelling. Error bars for M_D are shown in 2, while the uncertainties in r_0, v_{0h}, $R_{opt} \equiv 3.2R_D$ and ρ_0 amount to 30%, 15%, 15%, 40% respectively.

2.2 Photometry

From our optical/near-infrared imaging, we constrain the spectral energy distribution (SED) of each galaxy. Since the arcs usually lie with a few arcs-seconds of nearby bright cluster galaxies, we calculate the magnitude of the arcs in various pass-bands by masking the arc and interpolating the light from the nearby cluster members. The background light is then removed and surface photometry in different bands is obtained.

Using the cluster mass models the arcs are reconstructed to the source-plane and the geometry and disk-scale parameters of the disks are measured. This is achieved by fitting ellipses to an isophote of the galaxy image using a modified version of the IDL GAUSS2DFIT routine which fits an exponential profile to the two-dimensional light distribution. From this, the ellipticity, the inclination and luminosities and the disk scale lengths are obtained (see Table 2 and 3 in Swinbank et al. (2006)). These latter are also reported below in Table 1.

2.3 One-Dimensional Rotation Curves

In Fig. 1 we show the one dimensional rotation curves of the galaxies in our sample. These are extracted by sampling the velocity field along the major axis cross section. The zero-point in the velocity is defined using the center of the galaxy in the reconstructed source plane image. The error bars for the velocities are derived from the formal 3σ uncertainty in the velocity arising from Gaussian profile fits to the [OII] emission in each averaged pixel of the datacube. For the mass modelling analysis we folded the rotation curves on the kinematical center to ensure that any small-scale kinematical sub-structure is removed.

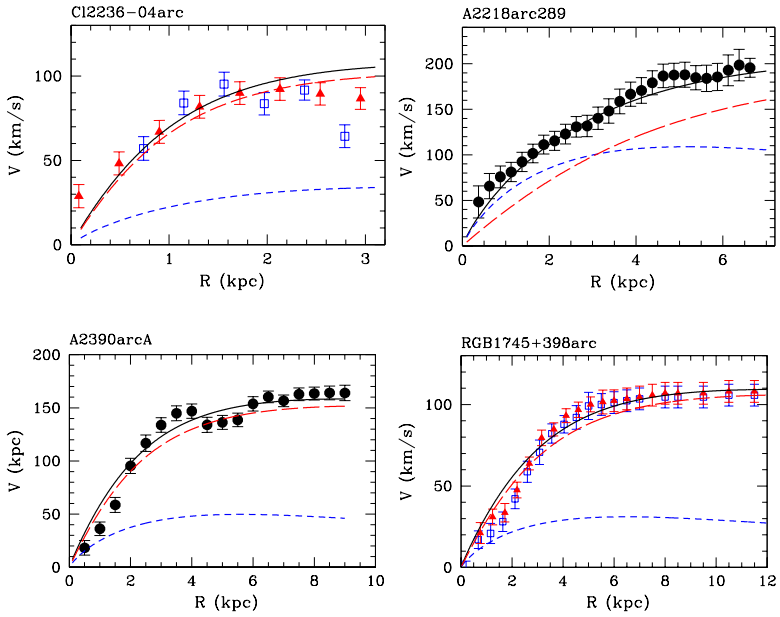

Figure 1. Filled circles represent the IFU rotation curves having enough data to allow the coaddition of the kinematics of the receding and the approaching arm, red and blue open circles represent the rotation curves along each arm in the other cases. The dark-matter and stellar components are shown with long dash and short dash lines, whilst the model circular velocity is shown with a solid line.

3 MODELLING AND RESULTS

The rotation curves of local spiral galaxies imply the presence of an invisible mass component, in addition to the stellar and gaseous disks. The paradigm is that the circular velocity field can be characterized by:

$$V^2 = V_D^2 + V_H^2 + V_{HI}^2 \qquad (1)$$

where the subscripts denote the stellar disk, dark halo and gaseous disk respectively. From the photometry we model the stellar component with a Freeman surface density (Freeman 1970):

$$\Sigma_D(R) = \frac{M_D}{2\pi R_D^2}\, e^{-R/R_D} \qquad (2)$$

where R_D is the disk lenght-scale, while $R_{opt} \equiv 3.2R_D$ can be taken as the "size" af the stellar disk, whose contribution to the circular velocity is:

$$V_D^2(x) = \frac{1}{2}\frac{GM_D}{R_D}(3.2x)^2(I_0K_0 - I_1K_1) \qquad (3)$$

where $x = R/R_{opt} \equiv R/(3.2R_D)$ and I_n and K_n are the modified Bessel functions computed at 1.6 x. In small spirals the HI disk is an important baryonic component only for $R > 3R_D$, i.e. outside the region considered here. It is plausible that in similar objects also at high redshifts, *inside* $3R_D$, the HI gas contributes to the gravitating baryonic mass by a very small amount, residing at larger radii and it slowly infalls forming the stellar disk.

For the dark matter component we take a spherical halo for which $V_H^2(R) = G\,M_H(< R)/R$. Following the observational scenario constructed in the local Universe (Persic & Salucci 1988; Salucci & Burkert 2000) we assume that it has the Burkert (1995) density profile (see also Salucci et al 2007):

$$\rho(R) = \frac{\rho_0\, r_0^3}{(R + r_0)\,(R^2 + r_0^2)}\ , \qquad (4)$$

where r_0 is the core radius and ρ_0 the effective core density. It follows that:

$$M_H(R) = k\left[\ln\left(1 + \frac{R}{r_0}\right) - \tan^{-1}\left(\frac{R}{r_0}\right) + \frac{1}{2}\ln\left(1 + \frac{R^2}{r_0^2}\right)\right] \qquad (5)$$

with $k = 6.4\,\rho_0\, r_0^3$ and of course $V_H^2(R) = GM_H(R)/R$ We note that the adopted velocity profile is a quite general: it allows a distribution with a core of size r_0, converges to the NFW profile at large distances and, for suitable values of r_0 can also mimic the NFW or a isothermal profile, over the limited region of galaxy which is mapped by the rotation curves.

The mass model has three free parameters: the disk mass M_D, the core radius r_0, and the central core density ρ_0. The observations extend out approximately $(2-3)R_D$, have 10-60 independent measurements with an observational error of $3\%-10\%$ in their amplitude, of 0.05-0.2 in their slopes $dlogV/dlogR$. The error in the estimate of the disk inclination angles is negligible with respect to the above. These errors are (understandably) higher than those associated with the best quality local RC's and make it difficult to constrain the halo density profile $\rho(R)$. However, they are sufficiently small to yield a reliable value for the halo mass, the average density inside a reference radius, (which we chose to be $R_2 \equiv 2R_D$ so that $< \rho > \equiv M_H(R_2)/(4/3\pi R_2^3)$ and the disk mass and a reasonable estimate of the "core radius".

By reproducing the observed rotation curves with the models given by equations 1-5 we derive the best fit parameters for each galaxy and overlay the resulting mass model onto each rotation curve in Fig. 1. In Table 1 we report the main structural parameters: the disk mass, the halo core radius, ρ_0, the optical radius R_{opt} and $v_{0h} \equiv V_H(R_{opt})$, i.e. the halo contribution to circular velocity at the optical radius.

In all our rotation curves the *amplitude* and the *profile* of the stellar disk contribution can not reproduce the

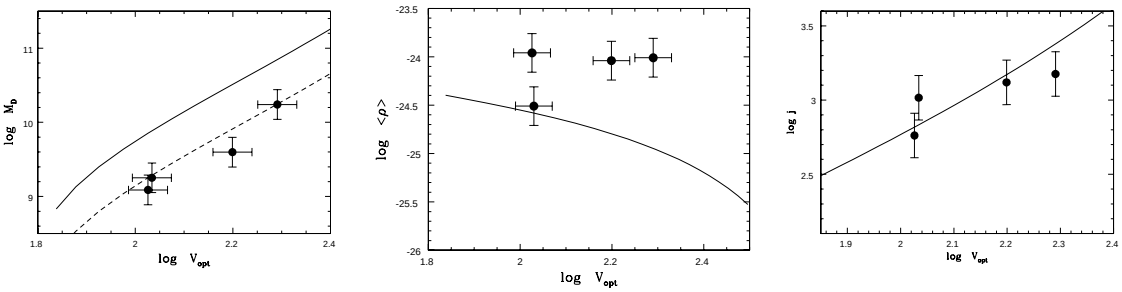

Figure 2. Left: disk mass (in solar units) versus reference velocity (in km/s) compared with the z=0 relation (*solid* line) and with this scaled down by 0.6 dex (*dashed* line). Middle: average dark matter density (in $g\ cm^{-3}$) versus reference velocity compared with the z=0 relation (*solid* line). Right: disk angular momentum per unit mass j (in $km/s\ kpc$ units) versus disk mass compared with the z=0 relation (*solid* line). The uncertainties on the local relations are: 0.15 dex in j, 0.2 dex in $\log M_D$ and 0.3 dex in $\log < \rho >$.

observed RC rise between 1.5 R_D and the last measured radius. This strongly suggests evidence for the presence, at $z \approx 1$, of a dark matter component of mass comparable to that found for local disk galaxies with similar V_{opt} (see Figures 2, 8 and 9 of Persic, Salucci & Stel, 1996). We derive disk masses ranging between $1 \times 10^9 M_\odot$ to $2 \times 10^{10} M_\odot$ for galaxies with reference velocity V_{opt} between $100\,\mathrm{km\,s^{-1}}$ and $200\,\mathrm{km\,s^{-1}}$. These disk masses are smaller by a factor 2-4 than those of the local spirals with the same reference velocity which are shown to follow Inner Baryon Dominance (see Salucci & Persic, 1999). The high redshift stellar disks are sub-maximal disks. Forcing a maximal disk even in the "weak" implementation of Persic and Salucci (1990) leads to unacceptable fits of our high-z RC's.

The best fit values for r_0 is of the order of $\sim 1.5 R_D$, which is larger than usually compatible with a NFW profile, although the error-bars on our data preclude any strong statement.

Since the gravitational lens model affects the source-plane reconstruction of the galaxies, we must test for the effect that this has on the resulting rotation curves. We reconstruct the galaxies using the family of lens models that inhabit the $\Delta\chi^2$ contour corresponding to 1σ confidence interval relevant to each cluster. For example, the model of RGB 1745 has five free parameters, and the lens modeling uncertainties are therefore derived by considering models within the $\Delta\chi^2$=5.89 contour. From each reconstruction we extract the one-dimensional rotation curve and apply the analysis outlined above and find the maximum variations are: $\Delta \log\ M_D = 0.03$, $\Delta \log < \rho >= 0.02$, $\Delta \log(V_{opt}) \lesssim 5\,\mathrm{km\,s^{-1}}$. Thus the uncertainties in the gravitational lens modelling is negligable compared to the uncertainties in the RC mass modelling.

A cosmological significance of our result is evident in Fig 2 where we compare the disk mass, the mean dark matter density within the optical radius and the angular momentum per unit mass, all as a function of reference velocity. These are compared to similar properties of the local objects (Shankar et al. 2006). Figure 2 strikingly shows that high redshift spirals, modulo an offset of $0.6^{+0.1}_{-0.15}$ dex, are on the same $logM_D$ versus $logV_{opt}$ relationship found for local spirals arising from the systematic structural properties of their mass distribution (Tonini et al. 2006), see also (Salucci et al. 1993) .

In Fig 2, from the values of $< \rho >$, a quantity that differently from ρ_0 is weakly affected by the RC 1-σ fitting uncertainties, it is apparent that the DM halos of $z = 1$ disk galaxies are denser by $0.7^{+0.1}_{-0.2}$ dex than those around similarly luminous z=0 spirals. The evidence that spiral disks at z=0 and z=1 have the same structural relationships is further supported by observations of the evolution of the Tully-Fisher relation (which correlates the disk mass with V_{opt}). In our and in other independent samples (Swinbank et al 2006, , Vogt et al 1996, Bamford et al 2005) the galaxies at $z = 1$ show a TF relation with a slope similar to that of the local TF, but with an offset compatible with that found in the present work from the disk mass *vs* rotation velocity. This suggests that from z=1 to z=0, the stellar disk masses M_D of a spiral has grown by a factor $\sim 4^{+1}_{-2}$, that leads to just a modest increase in the DM dominated quantity V_{opt} .

Further evidence that $z = 1$ disk galaxies are related to present day spirals is provided by the relationship between angular momentum per unit mass (j) versus the reference velocity, as shown in Fig. 2. This well theoretically motivated relation (e.g. (Tonini et al. 2006)) can be considered as the imprint of the process of the formation of disks inside dark matter halos related to the cosmological properties of halo spin parameters. As Figure 2 shows, there appears to be no evolution in this crucial relationship between the the comological time at which we observe these spirals, $z = 1, t = 6\ Gyr$ and the present time, $z = 0, t = 13.7\ Gyr$. This agreement is remarkable: it establishes a link between local and high redshift disks, supporting the idea that the angular momentum remains constant during the evolution of a disk system from high redshift to the present day.

The kinematical estimate of the disk mass allows us to derive the mass-to-light ratios for our disk systems as a function of luminosity and colour. In Fig. 3 we compare the disk mass and colour as a function of mass-to-light ratio compared to the relation in local spirals (Shankar et al. 2006). In order to compare directly with local relations, we consider a simple passive evolution model for the luminosity evolution. For a single stellar population the zero-point of the local relation is decreaed by a factor $log(13.7/6)$ which ac-

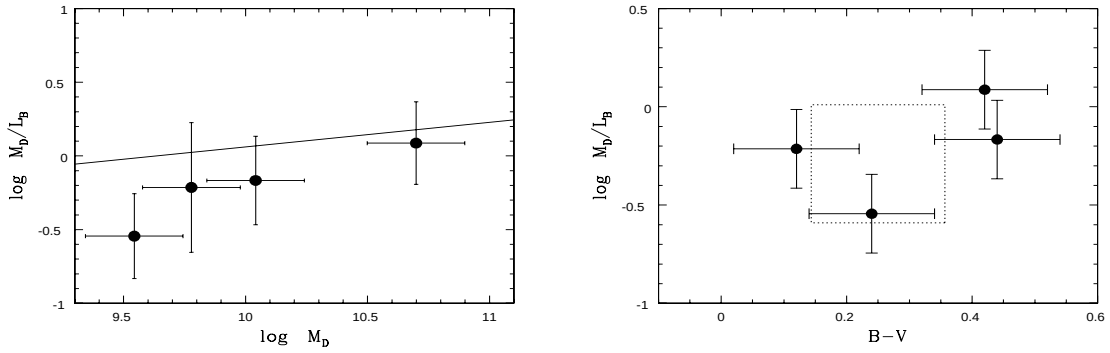

Figure 3. *Left:* Mass-to-light ratio versus disk mass for the galaxies in our sample compared with the local disk galaxies from Shankar et al. (1996) (solid line). The average offset corresponds to an excess in luminosity by a factor four. *Right:* Mass-to-light ratio versus colors relations for our sample. The square box denotes the predicted colours from a Bruzual & Charlot single stellar population (see text for details).

counts for the passive evolution of a *single* stellar population from $z = 1$ to $z = 0$. As Fig. 3 shows the mass-to-light ratios as a function of galaxy $(B - V)$ colour are in broad agreement with predictions of a single stellar population which is $\sim 1Gyr$ old (Bruzual & Charlot 2003), although clearly photometry at other wavelengths (such as rest-frame K-band) would allow a more detailed decomposition of the stellar popultations in these galxies.

3.1 Cosmological Implications

Figure 2 shows that at a radius corresponding to V_{opt} the high redshift galaxies are significantly denser than comparably luminous local disk-galaxies: the average offset is about 0.6 dex in $log(< \rho) >$. Although we can not exclude that dynamical processes occur between $z = 1$ and $z = 0$ to reduce the dark-matter density in the luminous regions, this offset is naturally explained if the halos embedding these disk galaxies formed at earlier times than the halos around similarly massive $z = 0$ spirals. In this framework we estimate the ratio between the virialization redshift of the local galaxies and and that of the galaxies in our sample. Since $\rho_v \propto \Delta(z_v)(1 + z_v)^3$ where ρ_v and z_v are average density and redshift at virialization and Δ_v is known, for $z_0 = 1$, $z_v = 1.7$, which corresponds to $t_v = 6\ Gyr$.

Assuming that our sample is a fair representation of disk galaxies at $z \sim 1$ and that these are approximately coeval, from the comparison of their structural properties with those of $z = 0$ spirals, the following simple picture emerges: a present day spiral, with a given circular velocity, half-light radius and the angular momentum per unit mass, at redshift 1 had similar values for these quantities, but a smaller stellar mass: $< M_\star(t_{obs})/M_\star(t_0) > \simeq 0.3$. This induces a scale for the average SFR in the past 8 Gyr: $\sim\ 0.75M_\star(t_0)/(t_{obs} - t_0) \sim\ 1(M_\star(t_0)/(10^{10}M_\odot)M_\odot/yr$. With these disks having an average age of 1 Gyr at $z = 1$ we can also derive an "early times" average SFR $\sim\ 0.25M_\star(t_0)/(1Gyr) \sim 3(M_\star(t_0)/(10^{10}M_\odot)M_\odot/yr$ which points towards a declining SFR history.

The marked increase of the luminosity per unit stellar mass in objects at high redshifts with respect to their local counterparts has the simplest explanation in a passive evolution of the starforming disks. Obviously, this simple picture requires us to assume that the high redshift systems are the direct counter-parts of similar rotation speed spirals at low redshift.

4 DISCUSSION AND CONCLUSIONS

In this study, we have investigated the detailed properties of four disk galaxies at $z = 1$. These galaxies were observed at high spatial resolution thanks to the boost in angular size provided by gravitational lensing by foreground massive galaxy clusters and allow a much more detailed comparison with local populations than usually possible for galaxies at these early times. Modelling the one-dimensional rotation curves with those of Persic et al. (1996) we derive best fit parameters for the total dynamical mass, the core radius, the effective core density and the angular momentum per unit mass.

The best fit model rotation curves to the data show that the amplitude and profile of the stellar disk componentcan not unambiguously reproduce the rise in the rotation curve without a dark matter component. Comparing the average dark matter density inside the optical radius we find that the disk galaxies at $z = 1$ have larger densities (by up to a factor of ~ 7) than similar disk galaxies in the local Universe. In comparison, we find that the angular momentum per unit mass versus reference velocity is well matched to the local relation suggesting that the angular momentum of the disk remains constant between high redshift and the present day. Though statistically limited, these observations point towards a spirals' formation scenario in which stellar disk are slowly grown by the accretion of angular momen-

tum conserving material. Our result, also consistent with the theoretical evolution of the angular momentum of disks from semi-analytic models from z=1 to z=0 which show the modest offset of $\Delta j \lesssim 0.2$ kpc. km s^{-1} for objects with circular velocities between 50 and 300 km s^{-1} (Cole et al. (2000); Bower et al. (2006)). These reults provide an evolutionary link between the disk systems we observe at redshift $z \sim 1$ and the present day population of spirals.

While these results are based on data of only four objects, they nevertheless show the power which gravitational lensing can have on studying the internal properties of high redshift galaxies. In particular, these observations should be viewed as pathfinder science which will soon be routine with Adaptive Optics Integral Field Unit observations on eight and ten meter telescopes (e.g. Genzel et al. 2006). Moreover, by combining these results with upcoming telescopes and instruments (e.g. ALMA) which will be sensitive enough to map the HI content of galaxies to $z = 1$, the exact relation between gas, stars and dark matter can be probed in much more detail.

ACKNOWLEDGMENTS

We would like to thanks the anonymous referee for his/her suggestions which improved the content and clarity of this paper. We thank Carlton Baugh for providing the theoretical evolution of disk mass in galaxies from GALFORM. We also thank Gigi Danese for useful discussions. AMS acknowledges support from a PPARC Fellowship, RGB acknowledges a PPARC Senior Fellowship and IRS and GPS acknowledges support from the Royal Society.

REFERENCES

Bamford, S. P., Milvang-Jensen, B., Aragón-Salamanca, A., & Simard, L. 2005, MNRAS, 361, 109
Bosma, A. 1981, AJ, 86, 1825
Bower, R. G., Benson, A. J., Malbon, R., Helly, J. C., Frenk, C. S., Baugh, C. M., Cole, S., & Lacey, C. G. 2006, MNRAS, 659
Bruzual, G. & Charlot, S. 2003, MNRAS, 344, 1000
Burkert, A. 1995, ApJL, 447, L25
Cole, S., Lacey, C. G., Baugh, C. M., & Frenk, C. S. 2000, MNRAS, 319, 168
Freeman, K. C. 1970, ApJ, 160, 811
Genzel, R., Tacconi, L. J., Eisenhauer, F., Förster Schreiber, N. M., Cimatti, A., Daddi, E., Bouché, N., & Davies, R., et al. 2006, Nature, 442, 786
Kneib, J.-P., Ellis, R. S., Smail, I., Couch, W. J., & Sharples, R. M. 1996, ApJ, 471, 643
Persic, M. & Salucci, P. 1988, MNRAS, 234, 131
Persic, M., & Salucci, P. 1990, MNRAS, 247, 349
Persic, M., Salucci, P., & Stel, F. 1996, MNRAS, 281, 27
Rubin, V. C., Thonnard, N., & Ford, Jr., W. K. 1980, ApJ, 238, 471
Salucci, P., Frenk, C. S., & Persic, M. 1993, MNRAS, 262, 392
Salucci, P. & Burkert, A. 2000, ApJL, 537, L9
Salucci, P., & Persic, M. 1999, A&AP, 351, 442
Shankar, F., Lapi, A., Salucci, P., De Zotti, G., & Danese, L. 2006, ApJ, 643, 14
Smith, G. P. 2002, Ph.D. Thesis, University of Durham, UK
Smith, G. P., Kneib, J.-P., Smail, I., Mazzotta, P., Ebeling, H., & Czoske, O. 2005, MNRAS, 359, 417
Swinbank, A. M., Bower, R. G., Smith, G. P., Smail, I., Kneib, J.-P., Ellis, R. S., Stark, D. P., & Bunker, A. J. 2006, MNRAS, 368, 1631
Swinbank, A. M., Smith, J., Bower, R. G., Bunker, A., Smail, I., Ellis, R. S., Smith, G. P., & Kneib, J. P., et al. 2003, ApJ, 598, 162
Tonini, C., Lapi, A., Shankar, F., & Salucci, P. 2006, ApJL, 638, L13
Vogt, N. P., Forbes, D. A., Phillips, A. C., Gronwall, C., Faber, S. M., Illingworth, G. D., & Koo, D. C. 1996, ApJL, 465, L15